Online pulp condition monitoring for abnormal event detection and long-term monitoring

Haasbroek, A.L.*, Auret, L.*, Muchima, Y.**

**Stone Three, Paardevlei, Cape Town, South Africa (lidia.auret@stonethree.com; attie.haasbroek@stonethree.com)*

****FQM Kansanshi (Yihemba.Muchima@fqml.com)*

Abstract: Varying feed conditions, operational challenges, changing mineralogy and suboptimal reagent dosing can cause abnormal and undesirable events that destabilize and reduce flotation performance. An industrial case study (copper concentrator) on the use of real-time pulp measurements to detect abnormal events and aggregate their impact on flotation performance to support early intervention by metallurgists is presented. Since mechanisms of flotation in the pulp and froth phases are complex, multivariate, and sensitive to disturbances, the availability of real-time pulp bubble measurements can provide valuable information on flotation performance to allow timely corrective actions. Online pulp sensors in a copper concentrator plant were validated through step tests, and historical data analysis shows the potential of flotation performance monitoring with these sensors. A pulp performance monitoring dashboard has been deployed to the copper concentrator. Events detected include sub-optimal frother dosing and abnormal mineralogy (e.g., carbonaceous material).

1. INTRODUCTION

Flotation typically represents the first separation step in mineral processing, where valuable minerals are potentially discarded to tailings facilities, e.g., up to 20% metal losses in platinum group metals processing (Gibson et al., 2023). Flotation performance management through automated control and monitoring is essential to minimize these losses (maximize recovery) while ensuring the required minimum concentrate grade, within the equipment constraints represented by the flowsheet.

Flotation separation mechanisms are complex, taking place in the pulp and froth phases in a flotation cell. In the pulp phase, surface attachment of valuable hydrophobic minerals is desired (with frother reagent used to ensure high bubble surface area to volume ratios) to ensure sufficient transport of valuable minerals to the pulp-froth interface. Pulp condition indicators such as pulp bubble size, gas holdup and superficial gas velocity are important metrics for flotation performance in the pulp. In the froth phase, a balance between froth residence time as well as froth stability must ensure sufficient opportunity for undesired entrained gangue to drain back to the pulp phase, while allowing valuable minerals to report to the cell concentrate. Frother reagent affects the froth stability, while air addition and pulp level affects the froth residence time. Froth condition indicators such as froth bubble size, froth velocity, and bursting rate are important metrics for flotation performance in the froth.

Extensive research has been conducted on the use of computer vision methods for froth measurement (see Aldrich et al., (2022) for a recent survey on froth computer vision), with several commercial froth sensors available. Real-time measurement of pulp conditions is an emerging industrial application: Horn et al. (2022) compared online and offline pulp sensor metrics in an industrial application, while Nienaber et al. (2022) investigated dynamic responses of online pulp metrics to step tests.

Pulp and froth conditions are sensitive to manipulated input variables (air addition valves, cell tails valves, reagent addition) and disturbance variables (composition and liberation of minerals, solids percentage, particle size, process water characteristics, feed rate, etc.). Of particular interest in this work, frother reagent affects the pulp phase (preventing coalescence of bubbles to ensure maximum bubble surface to volume ratio) as well as the froth phase (stabilising the froth to reduce bubble burst rate and excessive drainage). Optimal frother dosing should preferably be dynamic due to changing process conditions. However, frothers are typically ratio controlled to mill feed rate. Frother concentration in any cell can change due to losses (evaporation) and recirculation, and the measurement of frother concentration in a flotation cell is an unresolved challenge. The optimal frother dosage (critical coalescence concentration, or CCC) varies with air addition, pulp viscosity, and other effects.

The availability of real-time pulp condition measurements will allow online abnormal event detection, as well as long-term flotation performance monitoring, with potential application to optimizing frother and other reagent dosing. This paper demonstrates such flotation performance monitoring, as developed for an industrial copper concentrator. An overview of important pulp and froth measurements is provided in Section 2, while factors affecting these measures are discussed in Section 3. Section 4 gives a description of the industrial process and the methodology of this study, with results presented in Sections 5 and 6.

2. PULP AND FROTH MEASUREMENTS RELEVANT TO FLOTATION PERFORMANCE

Separation in a flotation cell is achieved by the attachment of hydrophobic mineral particles to air bubbles in the pulp phase (true flotation), the transport of these loaded bubbles to the pulp-froth interface, and the transfer of such mineral particles through the froth phase over the flotation cell lip as concentrate. Note that mineral particles, regardless of their hydrophobicity can also be transported through entrainment to the froth phase. The true flotation separation process can be modelled as a first-order kinetic process:

$$\dot{M}_{C,i} = k_i M_{P,i}$$

Where $\dot{M}_{C,i}$ [ton/s] is the mass flow rate of component i due to true flotation in the concentrate stream, k_i [1/s] is the kinetic rate, $M_{P,i}$ [ton] is the mass of component i in the pulp phase. The kinetic rate can be approximated according to the floatability component model (FCM) (Alexander et al., 2000):

$$k_i = P_i S_b R_f$$

Where P_i, the floatability parameter, is the probability of component i attaching to a bubble, S_b is the bubble surface area flux, and R_f is the froth recovery factor. P_i represents the likelihood of true flotation for component i, and can be modified through activator, collector and depressant reagents. S_b represents the pulp phase bubble attachment potential, while R_f represents the likelihood that a component that reports to the pulp-froth interface will be transported over the cell lip. S_b is calculated from the superficial gas velocity j_g and the Sauter mean pulp bubble size d_{32}.

$$S_b = \frac{6 j_g}{d_{32}}$$

j_g represents a normalized (according to cross-sectional area of the cell, A) air addition metric:

$$j_g = \frac{Q_{air}}{A}$$

From the above, important pulp measurements related to flotation performance are bubble size d_{32}, superficial gas velocity j_g and bubble surface area flux S_b. R_f captures the losses due to detachment and drainage in the froth phase, and is dependent on the froth residence time τ_f for air (Gorain et al., 1998):

$$R_f = \exp(-\beta \tau_f)$$

$$\tau_f = \frac{V_{froth}}{Q_{air}} = \frac{FD + FH}{j_g}$$

Where FD is the froth depth below the lip, and FH is the froth height above the lip. As bubbles travel from the pulp-froth interface to the top of the froth, bubble growth (dependent on τ_f and d_{32}) occurs such that the top-of-froth bubble size d_f is approximated by (Quintanilla et al., 2021):

$$d_f = \left(nC\tau_f + d_{32}\right)^{\frac{1}{n}}$$

The velocity of the froth flow over the lip v_f is related to the mass flow of the concentrate (due to true flotation and entrainment), as well as to the froth height over the lip and the gas holdup in the froth. From the previous, important froth measurements are froth velocity v_f and top-of-froth bubble size d_f.

3. FACTORS AFFECTING PULP AND FROTH CONDITIONS

Factors that affect pulp rheology impact pulp bubble size, and therefore S_b, with a knock-on effect on true flotation. Examples of such factors include solid concentration, carbonaceous material content, clay content, and pH modifiers such as lime.

Carbonaceous material may be associated as gangue with sulfide ores. Carbonaceous material negatively affects the flotation of valuable minerals – for example, some carbonaceous materials have large surface areas (associated with complex pore structures) as well as aromatic ring systems, adsorbing collector and resulting in excessive consumption of flotation reagents (Pan et al., 2022). Carbonaceous material may also affect pulp rheology (Hoang et al., 2018).

The presence of clay minerals was shown to increase pulp viscosity, by up to a factor of three for an increase of 0 to 15 wt% of clay content in a copper-gold ore (Zhang and Peng, 2015). Zhang and Peng (2015) also showed that high pulp viscosity resulted in lower copper recovery (up to 20% drop in recovery for 0 to 15 wt% clay content increase). Clay particles are typically small, being more prone to entrainment. Very fine clay minerals in the froth may stabilize the froth, increasing R_f. Furthermore, clay minerals have a large active surface area which cause more consumption of flotation reagents (Oats et al., 2010). In the case of frother this may negatively impact pulp bubble size. Zhang and Peng (2015) suggest remedial strategies for high clay content ores: blending, decreasing solid concentration, adding viscosity modifiers, or removing clay slimes before flotation.

Lime (typically added to flotation circuits to control pH) has been shown to impact pulp viscosity due to the presence of Ca^{2+} ions inducing the formation of particle aggregations, which increase viscosity (Wang and Li, 2020).

Nesset et al. (2012) derived a correlation for the effect of frother type (characterized by its critical coalescence concentration CCC [ppm]) and concentration ($C_{frother}$ [ppm]), superficial gas velocity (j_g [cm/s]), and relative viscosity (μ_r [-]) on pulp bubble size (d_{32} [mm]), based on lab scale equipment, and validated the approach on measurements from five industrial flotation plants. A simplification of this correlation (excluding gas density effects) is given by:

$$d_{32} = \mu_r^{0.776} \varphi(j_g, C_{frother}, CCC)$$

$$\varphi = 0.267 + f_l + 0.064(100 j_g)^{0.5} + \left(2.316 - (f_l + 0.267) + 0.0619(100 j_g)^{0.5} \exp\left(-3.09 \frac{C_{frother}}{CCC}\right)\right)$$

$$f_l = 0.0176(10.06 - CCC)$$

Figure 1 depicts the effect of $C_{frother}$, j_g and μ_r on d_{32} for a specific frother with $CCC = 5$.

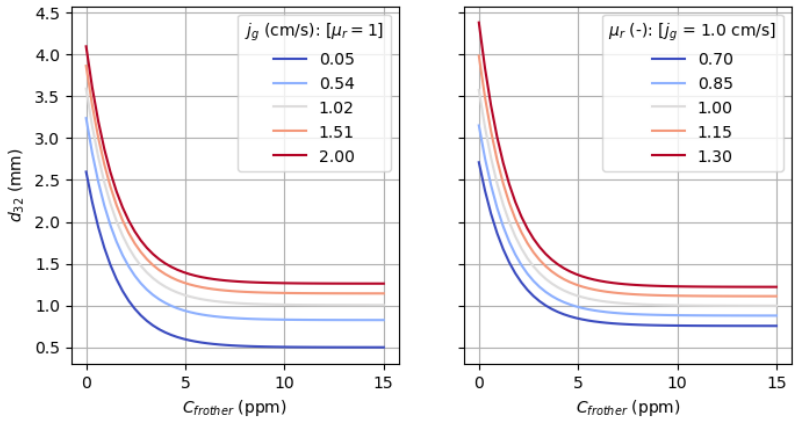

Figure 1: Effect of frother dose, superficial gas velocity, and relative viscosity on pulp bubble size according to the Nesset correlation.

3. PROCESS DESCRIPTION

Online pulp and froth sensors were installed at a copper plant that treats so-called sulphide, oxide and mixed ores (each in their own dedicated concentrator). Based on the complex geological characteristics of the mine, the feed grade to the concentrator plant is highly variable – with ore grades to the plant varying from 0.3% to 3.0%, causing considerable upsets to plant operation, and the potential of over- and underdosing of reagents (Ngulube et al., 2018). The sulphide ore typically has low clay content, while the oxide ore has very high clay content (Kalichini, 2015). High levels of carbonaceous phyllites, organic carbon and pyrite in the ore are present, requiring specific depressants (e.g., lime for pyrite suppression) (Dominguez et al., 2024). Reported reagent dosing schemes for the sulphide circuit (Ngulube et al., 2018) discuss collector dosage according to feed grade and throughput, and frother dosage based on a baseline of frother to collector ratio of 1:1, with a 30% range variation around this ratio based on froth velocity measurements.

From an operational perspective, undesired events can occur that affect the hydrodynamics and separation performance in the sulphide circuit. Such events can last around one hour or even as long as a shift or more. One example of such an undesired event is a period of flotation feed containing high amounts of carbonaceous material, leading to (unwanted) increased mass pull with subsequent downstream overfeeding. Another type of undesired event is a sudden decrease in froth depth (dropping to below the cell lip, hence no concentrate production), which is associated with small or absent top-of-froth bubbles. Many root causes may result in below lip conditions, including excess lime, upstream mill instability leading to particle size distribution deviations, and the presence of clay. Intervention during such events involves adjusting mass pull based on a hierarchy of actions: air is first adjusted, followed by pulp level adjustments, and finally reagent adjustments (lime, frother and depressant). Additional information that guides the required intervention includes mineralogy (e.g., for high pyrite conditions, lime addition would not be reduced, but frother may be increased) and milling performance indicators.

Seven pulp and eleven froth sensors in the sulphide circuit are considered in this work, with sensors of interest shown in the excerpt of the flowsheet in Figure 2.

Measurements available from the online pulp sensor include: number of bubbles detected in sensor view N_b, Sauter mean bubble size d_{32}, and gas hold up ε_g, while froth velocity toward the lip v_f and mean froth bubble size d_f are logged by the online froth sensor. The physical placement of sensors (both froth and pulp) will have a direct impact on measurements. In the case of the froth sensor, a representative froth location needs to be selected. This is complicated by uneven launders, froth crowders, and lip build-up. For the pulp sensor, it is important to ensure the sensor is placed deep enough into the pulp to not detect any froth phase

bubbles, while being high enough not to be impacted by rotor flow disturbances. Figure 3 below shows this approximate pulp sensor location as well as image examples.

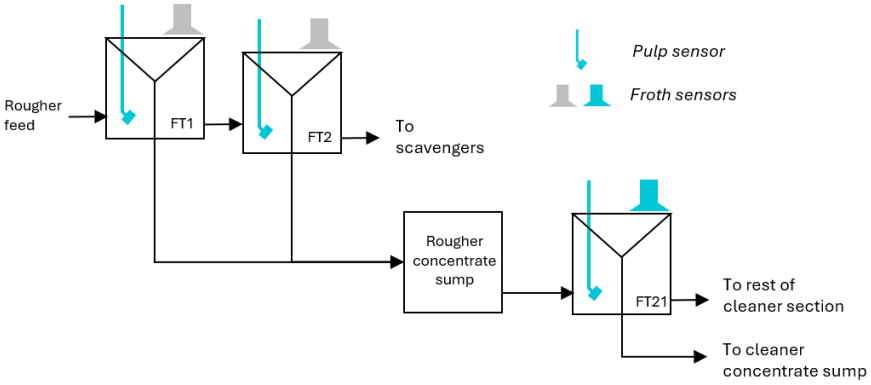

Figure 2: Excerpt of sulphide flotation circuit indicating location of pulp and froth sensors (Stone Three sensors indicated in indigo, other sensors in gray).

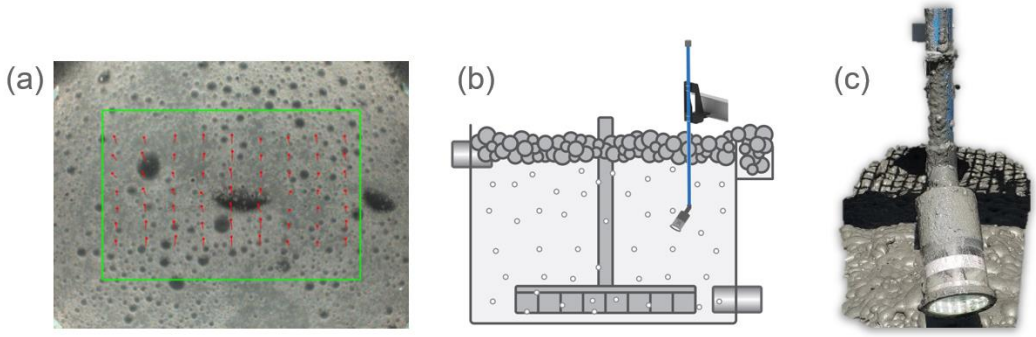

Figure 3: Pulp sensor example image (a), approximate installation depth, and (c) example of sensor before being submerged.

During installation of the pulp sensor, the vertical height was adjusted to determine the pulp froth interface depth with low pulp level set points. The sensors were then placed with a further safety margin. Figure 4 shows the corresponding pulp images which clearly show the difference as the sensor is placed deeper into the pulp. On the first image there is less pulp evident between the bubbles, and it resembles a froth structure. At 1000mm deeper the pulp is more visible with clear sections where no bubbles are seen.

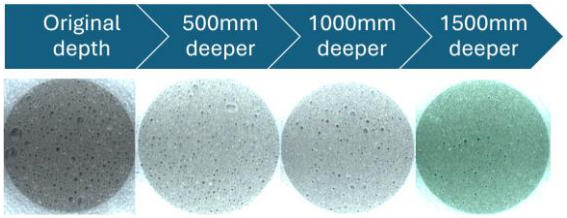

Figure 4: Comparison of bubble structure from pulp sensor view at varying depths from pulp interface.

The images in Figure 4 also provide a good reference when determining future image quality. If the bubble structure mimics the left most image one may deduce that the pulp level was too low for the sensor to provide sensible metrics.

4. STEP TEST TIME SERIES ANALYSIS

Step tests were done on site to confirm pulp sensor responses to frother reduction and air input changes. The first rougher cell FT01 was selected for frother steps, and the first four cleaner cells (FT21 - FT24) were selected for air steps.

In total, eighty set point adjustments were made over the course of three days. Data collected during this period includes more than 250 000 high resolution pulp and froth sensor images; more than 15 GB of time series metrics totaling more than 10 million samples; and 220 plant tags for context.

Live data and images were observed during the step experiments to confirm that a sufficient response is observed while ensuring process upsets are limited to an acceptable level. Figure 5 shows the data and images as observed in real time during the frother

reduction step on FT01. The reduction in number of pulp bubbles as well as the reduction in froth velocity over the lip is of interest. In this case, the step duration was decreased due to sufficient process response and to minimize recovery loss.

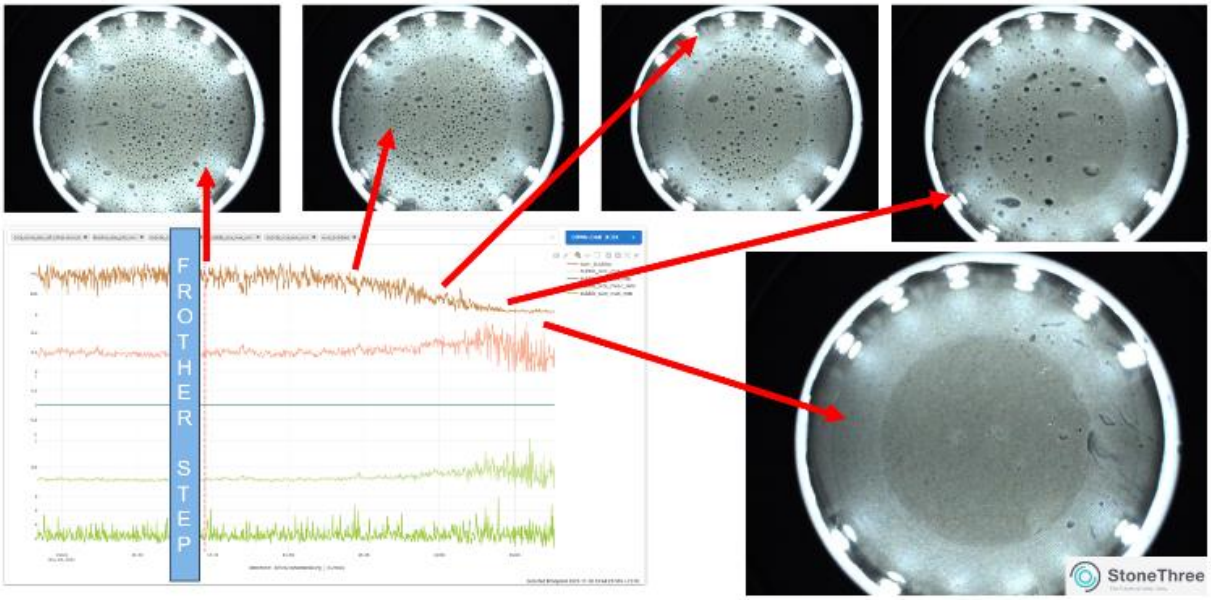

Figure 5: Live data and image view during frother steps.

Frother reduction on FT01

Pulp bubble size is expect to increase if frother is removed from the system (see Figure 1). In Figure 6, the frother flow is shown compared to pulp and froth metrics. Within 10 minutes of the frother being stepped to zero flow (point a at 13:50), the number of pulp bubbles start decreasing, with a 50 to a 100 times reduction in number observed within 30 minutes (point b).

Figure 7 shows the sensor images corresponding to each vertical line on the frother flow graph from Figure 6. A clear correlation between froth below lip, reduced number of pulp bubbles, and pulp bubble size distribution is seen.

The frother flow was increased at 14:10, resulting in an increase in pulp bubble count and decrease in pulp bubble size, as expected, stabilizing at 14:30. Air flow was increased at 15:30, followed by a decrease in the pulp bubble size at point c roughly 30 minutes later. The operators reacted by manually overriding the frother dosage (point d) and the process stabilized by 16:00. This series of events shows the importance of close collaboration with site metallurgists and operators to mitigate and correct process instabilities introduced by the step changes.

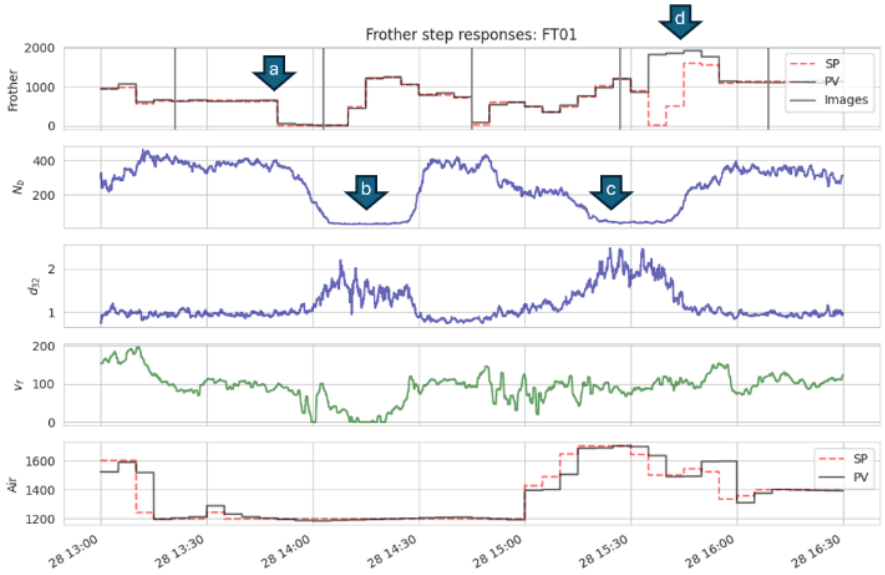

Figure 6: FT01 pulp and froth measurement response for step changes in frother addition setpoint. Points of interest: (a) Frother flow step to zero, (b) first period of reduced pulp bubbles, (c) second period reduced pulp bubbles, (d) frother flow switched to manual.

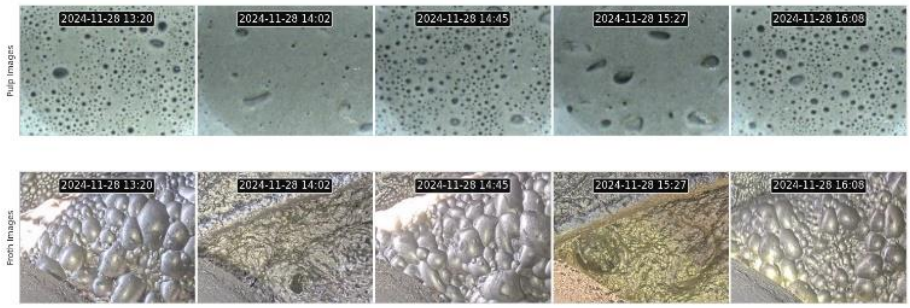

Figure 7: FT01 pulp and froth images corresponding to frother step experiment.

Abnormal event on FT01 detected before frother step

Prior to the frother step described above, a suspected frother depletion event was observed at FT01. It is not clear whether this was potentially due the presence of clay in the feed or a lime addition issue, both these causes being proposed by the site metallurgists. From the discussion in seciton 3 and the relatively flat pH trend in Figure 8 below the process response is consistent with an increase in clay content. Figure 9 shows the sensor images corresponding to each vertical line on the frother flow graph from Figure 8.

Furthermore, the pulp bubble size, pulp bubble count, froth velocity, and corresponding images show an almost identical response to those seen when reducing frother flow. Froth images between 12:30 and 13:00 confirm that the froth is below the cell lip – therefore concentrate production is limited during this time. This event highlights the importance of the pulp and froth measurements in highlighting the symptoms of a process upset.

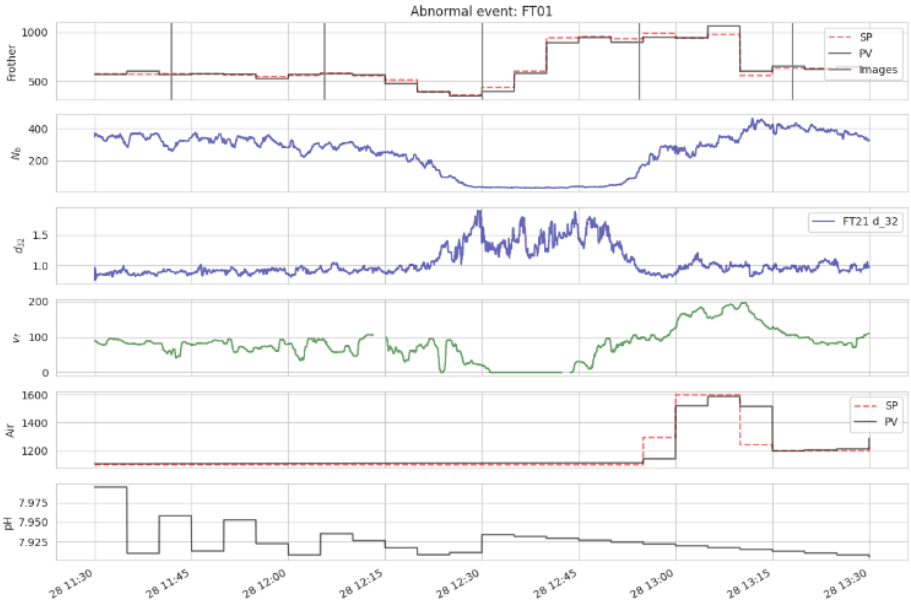

Figure 8: FT01 pulp and froth measurement response for an abnormal event.

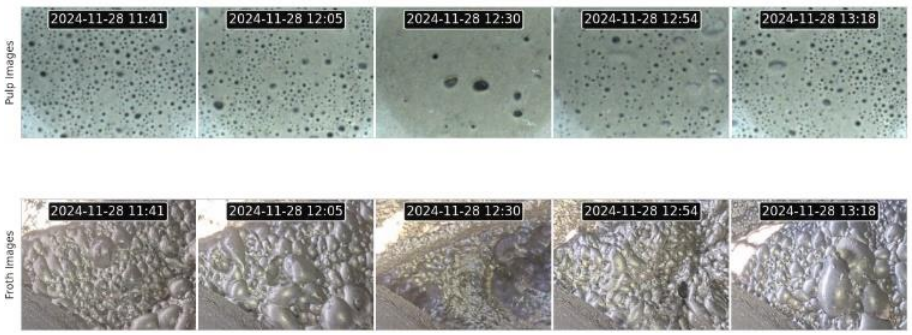

Figure 9: FT01 pulp and froth images corresponding to an abnormal event.

Historical data analysis

The previous results indicate significant pulp and froth measurement responses to frother and air manipulated variables, as well as responses to abnormal events. To determine the prevalence of pulp and froth abnormal events, historical data analysis was conducted on a longer period.

Data spanning 35 days between March and April 2025 was analyzed with expert rules to identify similar events on FT01, based on frother flow ($F_{frother}$), flotation feed flow (F_{feed}), number of pulp bubbles (N_b) and duration ($\Delta t = t_{end} - t_{start}$).

$$Event\ detected\ IF\ (\Delta t > 30\ min)\ \&\ t \in [t_{start}, t_{end}]:$$

$$F_{frother}(t) > 250\ \&\ N_b(t) < 100\ \&\ F_{feed}(t) > 3500$$

These rules aim to exclude process flow interruptions as well as no frother added events. Note that this is an initial search and would likely miss a significant number of events due to the conservative limits and the duration limit – in practice smaller events close to each other should be grouped into a single event.

Table 1 summarizes the identified events.

Table 1: Summary of detected abnormal events.

Event	Δt (h:m)	v_f	N_b	d_{32}	$F_{frother}$ SP	F_{air} SP	F_{feed}	Feed grade	Feed pH
#1	01:00	50.5	70	1.11	472	1700	3776	0.84	7.47
#2	00:58	26.1	78	1.04	339	2100	3772	0.69	7.83
#3	00:55	126.3	58	0.86	588	1900	3783	-	7.62
#4	00:48	31.5	70	1.07	716	2100	4165	1.3	7.53
#5	00:48	47.1	52	0.73	741	1750	4195	0.5	8.26
#6	00:36	151.1	42	0.74	1542	1500	4193	0.52	7.69
#7	00:35	19.9	87	1.31	684	2400	4238	0.48	8.18

After further investigation, event #3 was excluded due to erroneous feed grade data. Events #1 and #2 are discussed in more detail, with time series and images provided in Figure 10, Figure 11, Figure 12 and Figure 13.

Event #1 (Figure 10 and Figure 11) is similar to the abnormal event encountered during the step tests (Figure 8). The detection limits correctly identified the start and end times of the event. Event #2 (Figure 12 and Figure 13) is preceded by a period of low air addition. In this instance the detection limits did not identify the full duration of the potential abnormality, given the low pulp bubble count present before the detected event start time.

The pulp images in Figure 11 and Figure 13 show a distinct reduction in pulp bubble count. The Sauter mean size in Figure 10 and Figure 12 does not show as distinct an increase in all events.

5. MONITORING APPROACH

The previous section showed the response of the pulp and froth sensor measurements during planned step tests as well as normal process variations and abnormal events. Abnormal events may cause reduced process performance, since cell concentrate production may be reduced or halt during such events. A long-term, automated solution may be to include the pulp and froth metrics in automated control for handling (preventing and shortening) abnormal events. An interim approach is to monitor available measurements and report on sub-optimal conditions for the consideration of plant metallurgists and operators. Figure 14 provides a screenshot of the pulp and froth condition monitoring dashboard deployed on site.

The event detection rules used in the previous section to determine possible abnormal events were implemented as an analytical process that runs on demand on site, with a corresponding dashboard displaying monitoring results. Sub-optimal states are labelled according to symptomatic variables (e.g., “Large pulp bubble size”, “Low pulp bubble count”, “Unstable pulp bubble size” – the later based on monitoring rolling window mean changes). States of sensing issues such as “Stationary image” and “Sensor reading unavailable” are also reported. Relevant process data as well as pulp and froth images are shown to assist operators in troubleshooting unacceptable states.

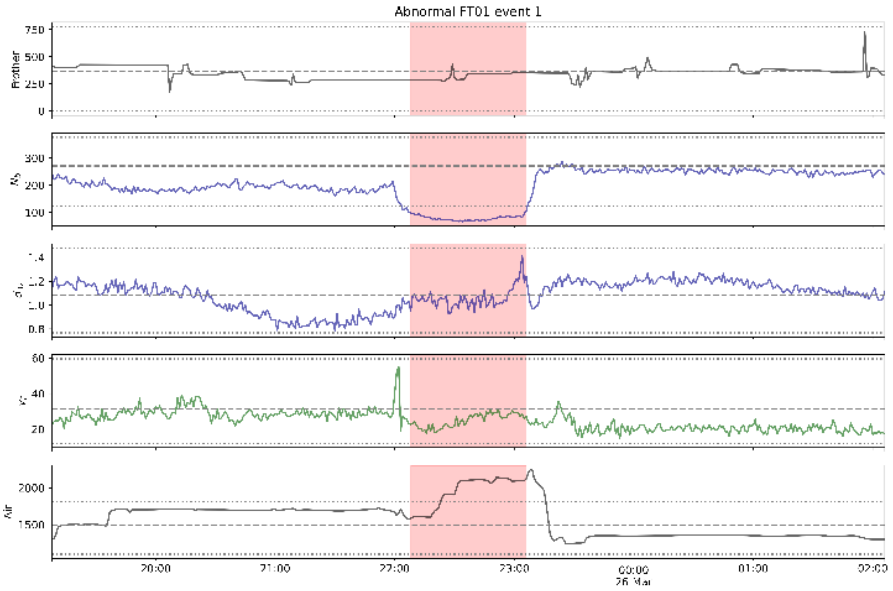

Figure 10: FT01 abnormal event #1 responses (highlighted in red) with preceding and subsequent time series included.

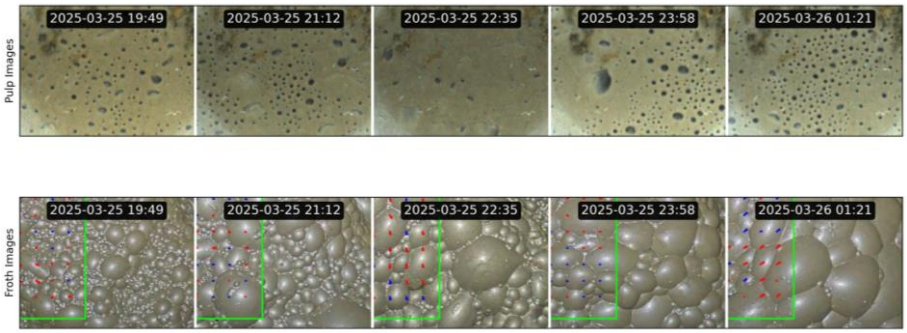

Figure 11: FT01 abnormal event #1 pulp and froth images.

Figure 12: FT01 abnormal event #2 responses (highlighted in red) with preceding and subsequent time series included.

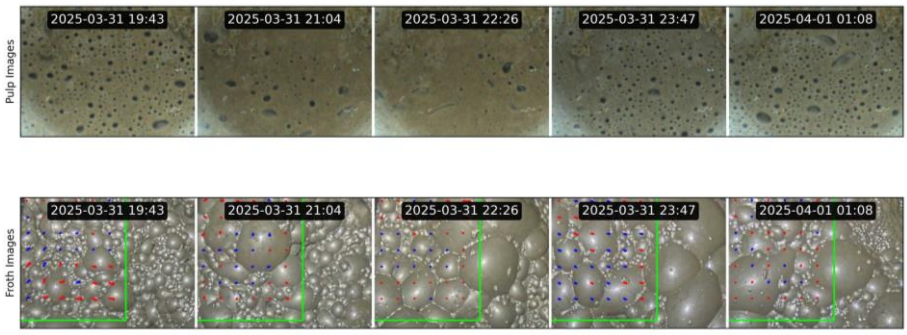

Figure 13: FT01 abnormal event #2 pulp and froth images

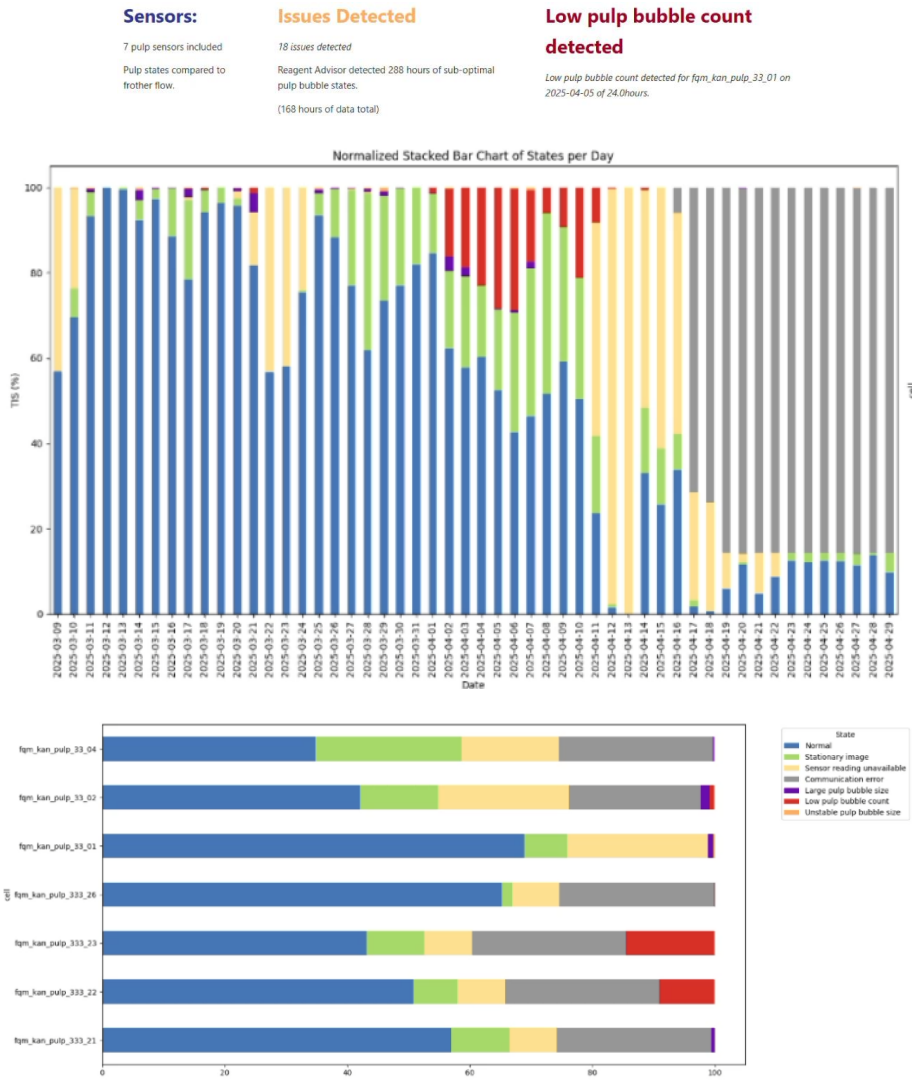

Figure 14: Deployed pulp condition monitoring dashboard

6. CONCLUSIONS AND FUTURE WORK

Pulp and froth conditions impact flotation plant performance. The ability to monitor pulp and froth conditions in real-time presents an opportunity for process monitoring and automated control solutions. This work has provided details on pulp sensor installation and testing in industrial conditions, with subsequent analysis of step test and abnormal event results, incorporating pulp and froth measurements. Details on the use of pulp measurements in a pulp condition monitoring dashboard deployed to site were also provided. The relation of these measurements to flotation separation was described through the theory of floatability component modelling (showing the impact of pulp and froth conditions on potential recovery through true flotation). The theoretical impact of various factors on pulp bubble size (an important true flotation driving force) was investigated through

an industrially calibrated correlation provided by Nessett et al. (2012), with pulp rheology factors such as clay mineralogy and process water quality discussed.

Future work includes the application of fault detection and classification algorithms (based on image and time series data) to further improve process monitoring of the pulp and froth conditions, as well as the development of an advisory system to recommend appropriate interventions timeously.

ACKNOWLEDGEMENTS

The authors would like to thank the operators and metallurgists at FQM Kansanshi for the co-operation and assistance provided during the work on this project, and the preparation of this manuscript. Nalco Ecolab is acknowledged for their financial and technical support.

REFERENCES

Aldrich, C., Avelar, E., Liu, X., 2022. Recent advances in flotation froth image analysis. Minerals Engineering 188, 107823. https://doi.org/10.1016/j.mineng.2022.107823

Alexander, D., Runge, K.C., Franzidis, J., Manlapig, E., 2000. The application of multi-component flotatability models to full-scale flotation circuits, in: Seventh Mill Operators' Conference, 177. Presented at the 7th Mill Operators Conference (MOC), AusIMM, Melbourne, Vic, p. 167.

Dominguez, C.G., Lawlor, M., Briggs, A., 2024. Kansanshi Operations (Technical Report No. NI 43-101). First Quantum Minerals, Zambia.

Gibson, B.A.K.K., Nwaila, G., Manzi, M., Ghorbani, Y., Ndlovu, S., Petersen, J., 2023. The valorisation of platinum group metals from flotation tailings: A review of challenges and opportunities. Minerals Engineering 201, 108216. https://doi.org/10.1016/j.mineng.2023.108216

Gorain, B.K., Harris, M.C., Franzidis, J.-P., Manlapig, E.V., 1998. The effect of froth residence time on the kinetics of flotation. Minerals Engineering 11, 627–638. https://doi.org/10.1016/S0892-6875(98)00047-8

Hoang, D.H., Kupka, N., Peuker, U.A., Rudolph, M., 2018. Flotation study of fine grained carbonaceous sedimentary apatite ore – Challenges in process mineralogy and impact of hydrodynamics. Minerals Engineering 121, 196–204. https://doi.org/10.1016/j.mineng.2018.03.021

Horn, Z.C., Haasbroek, A.L., Nienaber, E.C., Auret, L., Brooks, K.S., 2022. Comparison of online and offline pulp sensor metrics in an industrial setting. IFAC-PapersOnLine, 19th IFAC Symposium on Control, Optimization and Automation in Mining, Mineral and Metal Processing MMM 2022 55, 91–96. https://doi.org/10.1016/j.ifacol.2022.09.249

Kalichini, M.S., 2015. A study of the flotation characteristics of a complex copper ore (Masters Thesis). University of Cape Town, Cape Town.

Nesset, J.E., Zhang, W., Finch, J.A., 2012. A benchmarking tool for assessing flotation performance, in: 44th Annual Canadian Mineral Processor's Operators Conference. Presented at the 44th Annual Canadian Mineral Processor's Operators Conference, Canadian Mineral Processors, Ottawa.

Ngulube, C., Munalula, W., Mkandawire, I., 2018. Development of Automated Flotation Reagent System, in: Copper Cobalt Africa, Incorporating the 9th Southern African Base Metals Conference. Presented at the Copper Cobalt Africa, incorporating the 9th Southern African Base Metals Conference, 10 - 12 July 2018, Southern African Institute of Mining and Metallurgy, Livingstone, Zambia, pp. 163–172.

Nienaber, E.C., Brooks, K.S., Auret, L., 2022. Insights from dynamic models for an online flotation pulp sensor, in: 8th International PGM Conference. Presented at the 8th International PGM Conference, Sun City, 2 - 3 November 2022, Southern African Institute of Mining and Metallurgy, Sun City, South Africa, pp. 261–275.

Oats, W.J., Ozdemir, O., Nguyen, A.V., 2010. Effect of mechanical and chemical clay removals by hydrocyclone and dispersants on coal flotation. Minerals Engineering 23, 413–419. https://doi.org/10.1016/j.mineng.2009.12.002

Pan, Z., Xiong, J., Cui, Y., Wei, Q., Jia, W., Zhang, Z., Jiao, F., Qin, W., 2022. Effect mechanism of carbonaceous materials on the flotation separation of lead–zinc ore. Separation and Purification Technology 294, 121101. https://doi.org/10.1016/j.seppur.2022.121101

Quintanilla, P., Neethling, S.J., Navia, D., Brito-Parada, P.R., 2021. A dynamic flotation model for predictive control incorporating froth physics. Part I: Model development. Minerals Engineering 173, 107192. https://doi.org/10.1016/j.mineng.2021.107192

Wang, L., Li, C., 2020. A Brief Review of Pulp and Froth Rheology in Mineral Flotation. Journal of Chemistry 2020, 3894542. https://doi.org/10.1155/2020/3894542

Zhang, M., Peng, Y., 2015. Effect of clay minerals on pulp rheology and the flotation of copper and gold minerals. Minerals Engineering 70, 8–13. https://doi.org/10.1016/j.mineng.2014.08.014